

# A microscopic model for spontaneous fission: validity of the adiabatic approximation

K. Hagino<sup>1</sup> and G.F. Bertsch<sup>2</sup>

<sup>1</sup> *Department of Physics, Kyoto University, Kyoto 606-8502, Japan*

<sup>2</sup> *Department of Physics and Institute of Nuclear Theory, Box 351560,  
University of Washington, Seattle, Washington 98195, USA*

We investigate microscopically the tunneling dynamics in spontaneous fission of atomic nuclei. To this end, we employ a schematic solvable model with a pairing-plus-quadrupole interaction. The spontaneous decay of a system is simulated by introducing a small imaginary part to the energy of a fission doorway state. We show that the many-body Hamiltonian can be reduced to an effective  $2 \times 2$  Hamiltonian, from which one can derive a simple approximate formula for the decay width. We particularly investigate the applicability of the adiabatic approximation, which has often been used in the literature. With typical value of the parameters, we find that the adiabatic approximation may underestimate the decay width by orders of magnitude, depending on the number of orbital transitions.

## I. INTRODUCTION

Nuclear fission is a primary decay mode of heavy nuclei. It plays an important role in a diversity of phenomena, including nuclear technology, syntheses of superheavy elements, and r-process nucleosynthesis. While there has been much recent progress in the theory [1], its microscopic understanding is still far from complete. An adequate quantum description not only has to deal with the very large changes in shape, but also with huge number of many-body configurations that are involved in the transition. One of the ultimate goals of low-energy nuclear theory is to develop a microscopic framework to describe this complex dynamics. For that purpose, one would need an efficient truncation scheme in order to handle the problem within a manageable computation time.

Given this situation, it may be useful to consider solvable microscopic models to test the reliability of the approximations in current use, and perhaps even to suggest new approximation schemes. A good model should be simple, yet should contain the essential features of large-amplitude quantum dynamics. One of us (G.F.B.) has proposed a model along these lines, reported in Ref. [2]. There the model was applied to induced fission, that is, fission in a nucleus excited about the fission barrier. It was demonstrated in that paper that the branching ratio in the competition between the fission and the capture reaction is sensitive to the character of the residual interaction.

In this paper, we apply the model to spontaneous fission, but with Hamiltonian parameters adapted to that process. Here barrier penetration plays a decisive role and the barrier height can be controlled by one of the parameters. We shall apply the model to investigate the accuracy of the adiabatic approximation, which has often been employed in microscopic calculations for nuclear fission.

The paper is organized as follows. In Sec. II, we introduce the model Hamiltonian used in our investigations.

In Sec. III, by numerically diagonalizing the Hamiltonian matrix, we investigate the dependence of the decay width on several parameters in the model. In Sec. IV, we introduce the adiabatic approximation and discuss its applicability. We then summarize the paper in Sec. V. In Appendix A, we discuss an alternative way to solve the model Hamiltonian using a time-dependent approach.

## II. MODEL HAMILTONIAN

The model Hamiltonian introduced in Ref. [2] reads

$$\hat{H} = \sum_{k=0}^{N_{\text{orb}}-1} \epsilon_k \hat{n}_k + v_Q \hat{Q} \hat{Q} + \sum_{\bar{k}, k'} v_{k k'} \hat{P}_k^\dagger \hat{P}_{k'} \quad (1)$$

where  $\hat{n}_k = a_k^\dagger a_k + a_{\bar{k}}^\dagger a_{\bar{k}}$  is the number operator for orbital  $k$  including its time-reversed partner  $\bar{k}$ , and  $\epsilon_k$  is the single-particle energy of the orbital and its partner. The operator  $\hat{Q}$  represents a shape-dependent fields such as the quadrupole operator. It is defined as  $\hat{Q} = \sum_k q_k \hat{n}_k$ . Finally, the operator  $\hat{P}_k^\dagger = a_k^\dagger a_{\bar{k}}^\dagger$  creates a pair in one of the orbitals.

As in Ref. [2], we study the model in a configuration space containing  $N_p = 6$  particles in  $N_{\text{orb}} = 6$  orbitals. The orbitals are grouped by shape; the first three favor the ground-state shape and the last three the shape associated with the scission configuration. This is implemented with orbital quadrupole moments  $q_k = -1$  for the first three and  $q_k = 1$  for for the last three. Labeling the orbitals as  $(k = 0, 1, \dots, 5)$ , we set the single-particle energies  $\epsilon_k$  as

$$\epsilon_k = (k \bmod (N_{\text{orb}}/2)) \varepsilon_0 \quad (2)$$

where  $\varepsilon_0$  is the single-particle level spacing. Table I summarizes the single-particle energies and the quadrupole moment for each orbital. In Ref. [2] there was added a small random energy to break some unwanted degeneracies. In the application to barrier penetration, the only

TABLE I: The single-particle energy  $\epsilon_k$  and the quadrupole moment  $q_k$  for single-particle orbitals in the  $(N_{\text{orb}}, N_p) = (6, 6)$  model. The single-particle energies are given in units of  $\epsilon_0$

$k$	0	1	2	3	4	5
$\epsilon_k$	0	1	2	0	1	2
$q_k$	-1	-1	-1	1	1	1

degeneracy of consequence is between the end configurations. We shall deal with this by introducing a shift  $\Delta$  to the diagonal energy of the precission configuration.

The two-body interaction is taken to purely pairing in the form

$$v_{kk'} = -G(1 - \delta_{k,k'}). \quad (3)$$

With this interaction the seniority of the wave function is a good quantum number. Note that the diagonal matrix elements of the pairing Hamiltonian are set to zero. This does not affect the wave function and permits a better separation between the diagonal and off-diagonal parameterization in the Hamiltonian. We consider below only the seniority-zero subspace, namely configurations having 3 pairs in the 6 orbitals. The total number of configurations in the space is

$$N_{\text{conf}} = \binom{N_{\text{orb}}}{N_p/2} = 20. \quad (4)$$

We now discuss the choice of parameters. Physically the most relevant parameters in spontaneous fission by pairing dynamics is the barrier height  $V_B$  and the pairing gap  $\Delta_{\text{BCS}}$ . Typical physical values in the actinide nuclei are  $V_B \approx 5$  MeV,  $\epsilon_0 \approx 0.5$  MeV, and  $\Delta_{\text{BCS}} \approx 0.8$  MeV. The model has only two dimensionless parameters,  $v_Q/\epsilon_0$  and  $G/\epsilon_0$ , besides the size parameters  $N_{\text{orb}}$  and  $N_p$ . We will eventually vary the parameters, but for now take the shape dependence as

$$v_q = -0.3125 \epsilon_0. \quad (5)$$

The resulting spectrum of energies of the individual configurations is shown in Fig. 1.

There are four sets of configurations distinguished by their expectation values of the  $Q$  operator, with one configuration in the extreme sets and nine in the interior sets. The leftmost configuration is the main component of the ground state, while the rightmost one represents a doorway to the fission channels. These two configurations are degenerate in the model as so far presented. The energy gap between the ground state configuration and the lowest states in the interior configurations is  $V_B = 6\epsilon_0$ . This is lower than a typical physical barrier, but as mentioned earlier we will consider parameter variations over a broad range.

For the pairing interaction strength  $G$ , we compare with a physical pairing strength via the BCS approximation to the pairing gap. Here we carry out the BCS

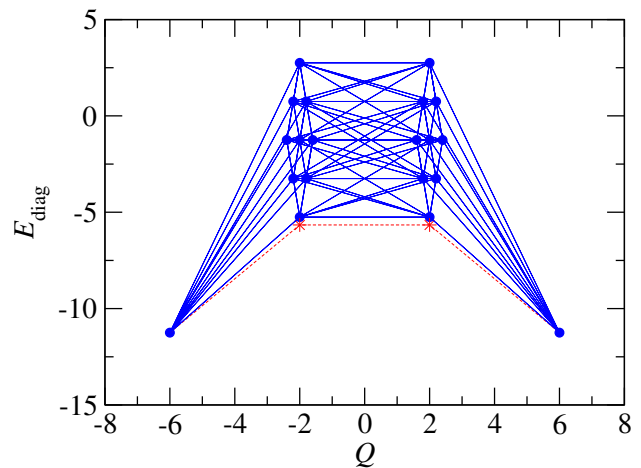


FIG. 1: Diagonal energies of the configurations in the  $(N_{\text{orb}}, N_p) = (6, 6)$  model space with shape parameter Eq. (5) are shown as the filled circles. The off-diagonal interaction connects configurations joined by lines. Stars show energies of adiabatic intermediate states; see Sec. IV for details.

calculation in a space of  $N_{\text{orb}}$  orbitals occupied by  $N_p/2$  pairs. For this calculation we assume that the orbital energies are evenly spaced by an energy difference  $\epsilon_0$ . For  $N_{\text{orb}} = 6$  and  $N_p = 6$ , an interaction strength of  $G/\epsilon_0 = 0.691$  produces the BCS gap of  $\Delta_{\text{BCS}}/\epsilon_0 = 3/2$ . This is close to the above rough estimate and we carry out the Hamiltonian calculations with it. Finally, we modify the diagonal energy  $E_d$  of the doorway configuration by adding a small imaginary part  $-i\Gamma_d/2$  and a small real part  $\Delta$ ,  $E_d = E_g + \Delta - i\Gamma_d/2$  where  $E_g$  is the energy of the leftmost configuration. The resulting non-Hermitian Hamiltonian is diagonalized to obtain a spectrum of decaying states. The decay width is given by

$$\Gamma_f = -2\text{Im} E_{gs}, \quad (6)$$

where  $E_{gs}$  is the eigenenergy of the state having the largest component of the leftmost configuration. The procedure will fail if the two end states are degenerate, because then there will be two candidates having nearly equal amplitudes for the configuration. We therefore have to understand the dependence of the calculated width on their (real) splitting  $\Delta$ . As we show below, the lack of specific knowledge of  $\Delta$  is not an obstacle to assess the adiabatic approximation.

### III. DECAY WIDTH

We now examine the dependence of the ground state decay width on the doorway width. This is shown in Fig. 2 for the offset  $\Delta = 0.1$  in the doorway energy. One sees that  $\Gamma_f$  first rises linearly with  $\Gamma_d$ , in accord with the first-order perturbation theory formula

$$\Gamma_f = \Gamma_d |\phi_d|^2 \quad (\text{perturbative}) \quad (7)$$

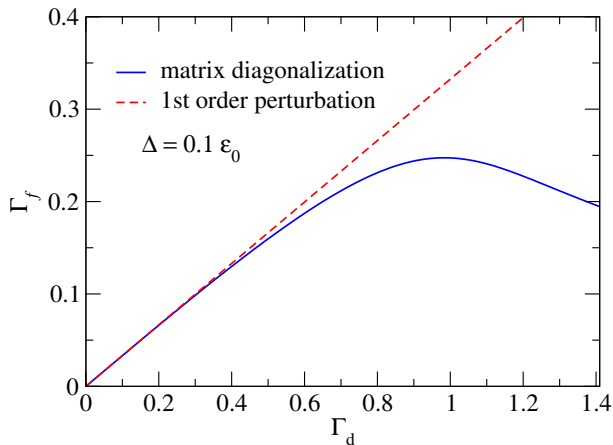


FIG. 2: The decay width of spontaneous fission,  $\Gamma_f$ , as a function of the width of the fission doorway state,  $\Gamma_d$ . These widths are given in units of  $\epsilon_0$ . The solid line is obtained by diagonalizing the non-Hermitian Hamiltonian for a system with 3 pairs in 6 orbits, while the dashed line is the result of the first order perturbation theory with respect to  $\Gamma_d$ .

where  $|\phi_d|^2$  is the probability of the doorway configuration in the unperturbed ground state. The region of validity of Eq. (7) is not broad enough for our purposes and we do not consider it further. Note that  $\Gamma_f$  saturates at larger  $\Gamma_d$  and then decreases. The decrease may be analogous to the phenomenon of super-radiance discussed e.g., in Ref. [3].

Since the offset is important to the calculation, it has to be fixed when comparing different Hamiltonian approximations. This can be achieved by reducing the Hamiltonian matrix to a  $2 \times 2$  matrix containing only the two end configurations. To achieve this, we divide the configuration space into three parts: the unperturbed ground state, the fission doorway, and all the interior configurations as the third part. Let us call the Hamiltonian for the interior configurations  $H_b$  (for “barrier”). The matrix elements coupling  $H_b$  to the end configurations will be designated  $\mathbf{v}_g$  and  $\mathbf{v}_d$ , where the bold-face type is a reminder that these are vectors with the same dimension as  $H_b$ . The Hamiltonian to be diagonalized has the form

$$H = \begin{pmatrix} E_g & \mathbf{v}_g^T & 0 \\ \mathbf{v}_g & H_b & \mathbf{v}_d \\ 0 & \mathbf{v}_d^T & E_g + \Delta - i\Gamma_d/2 \end{pmatrix}. \quad (8)$$

Here  $E_g$  and  $E_g + \Delta$  are the energies of the unperturbed ground state and the doorway state, respectively. The eigenvector for the decaying state satisfies the equation

$$\begin{pmatrix} E_g & \mathbf{v}_g^T & 0 \\ \mathbf{v}_g & H_b & \mathbf{v}_d \\ 0 & \mathbf{v}_d^T & E_g + \Delta - i\Gamma_d/2 \end{pmatrix} \begin{pmatrix} \phi_g \\ \phi_b \\ \phi_d \end{pmatrix} = E_{gs} \begin{pmatrix} \phi_g \\ \phi_b \\ \phi_d \end{pmatrix}. \quad (9)$$

If one knew the complex ground state energy  $E_{gs}$ , this equation could be solved for  $\phi_b$  as

$$\phi_b = (E_{gs} - H_b)^{-1}(\mathbf{v}_g \phi_g + \mathbf{v}_d \phi_d). \quad (10)$$

Substituting this to the original eigenvalue equation, one finds

$$H_{\text{eff}} \begin{pmatrix} \phi_g \\ \phi_d \end{pmatrix} = E_{gs} \begin{pmatrix} \phi_g \\ \phi_d \end{pmatrix}, \quad (11)$$

with

$$H_{\text{eff}} = \begin{pmatrix} E_g + v_{\text{eff},gg} & v_{\text{eff},gd} \\ v_{\text{eff},dg} & E_g + \Delta - i\frac{\Gamma_d}{2} + v_{\text{eff},dd} \end{pmatrix} \quad (12)$$

and

$$v_{\text{eff},ij} = \mathbf{v}_i^T (E_{gs} - H_b)^{-1} \mathbf{v}_j. \quad (13)$$

The reduction of the problem to the  $2 \times 2$  effective Hamiltonian is exact as long as the eigenenergy  $E_{gs}$  is correct. One can derive a simpler approximate Hamiltonian assuming that the fission barrier is much higher than other energies in the model. If  $E_{gs}$  is close to the unperturbed ground state energy,  $E_g$ , and the imaginary part is also small, we may assume  $E_{gs} \approx E_g$  in evaluating  $(E_{gs} - H_b)^{-1}$ . The second-order terms in the diagonal entries to the Eq. (12) are also small. In fact they are equal for the Hamiltonian Eq. (1). In effect, the diagonal terms only produce a shift in the total energy which can be ignored if it is small compared to  $V_B$ . The resulting approximate effective Hamiltonian can be written

$$H'_{\text{eff}} = \begin{pmatrix} E_g & v_{\text{eff}} \\ v_{\text{eff}} & E_g + \Delta - i\frac{\Gamma_d}{2} \end{pmatrix}, \quad (14)$$

with

$$v_{\text{eff}} = v_{\text{eff},gd} \quad (15)$$

To assess the accuracy of the approximations we made to derive Eq. (14), we compare with the exact second-order terms, Eq. (13). For parameters  $G$  and  $v_Q$  given in Sec. II in the numerical Hamiltonian, the second-order contribution to diagonal energies is  $-0.803\epsilon_0$ , which is indeed small compared to  $V_B$ . The effective interaction between the two end configurations is found to be  $v_{\text{eff}} = -0.260\epsilon$ . The corresponding quantity under the approximation  $E_{gs} \rightarrow E_g$  is  $v_{\text{eff}} = -0.348\epsilon$ . Although the difference from the exact is larger than we would like, it will factor out of the quantities we will use to test the adiabatic treatment.

We shall consider one additional approximation for calculating ratios. Under physical conditions,  $v_{\text{eff}}$  will be small compared to the other energies in Eq. (14), permitting one to estimate  $E_{gs}$  by second-order perturbation theory. This leads to

$$E_{gs} \approx E_g + \frac{v_{\text{eff}}^2}{-\Delta + i\Gamma_d/2}, \quad (16)$$

from which one obtains the decay width

$$\Gamma_f \approx \frac{\Gamma_d v_{\text{eff}}^2}{\Delta^2 + \Gamma_d^2/4}. \quad (17)$$

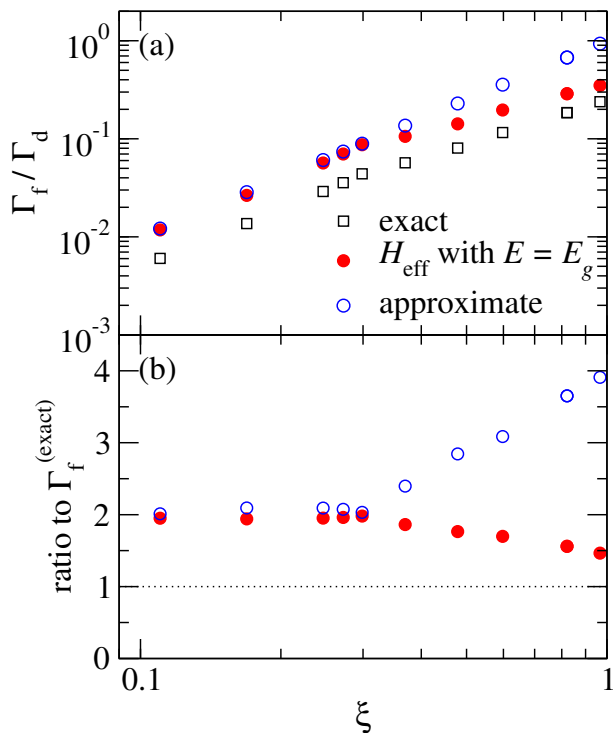


FIG. 3: The decay width obtained with several methods. It is plotted as a function of the parameter  $\xi \equiv -v_{\text{eff}}/\sqrt{\Delta^2 + \Gamma_d^2/4}$ , where  $v_{\text{eff}}$  is the off-diagonal coupling strength in the effective Hamiltonian, Eq. (14). For the exact results, shown as the open squares, the abscissa is the real part of  $\xi$ . The filled circles are obtained by the approximation  $E_{gs} \rightarrow E_b$  in the effective Hamiltonian Eq. (12). The open circles show the results of the approximate formula, Eq. (17). All energies are measured in units of  $\epsilon_0$ .

This subsumes the dependence on  $v_{\text{eff}}$ ,  $\Delta$  and  $\Gamma_d$  in a single dimensionless parameter

$$\xi \equiv -v_{\text{eff}}/\sqrt{\Delta^2 + \Gamma_d^2/4}. \quad (18)$$

We can now assess the accuracy of the approximations as a function of  $\xi$ . The comparison with the exact is shown in Fig. 3 as a function of  $\xi$ , but computed for a range  $[0.2 - 3.0]\epsilon_0$  of the  $\Delta$  and  $\Gamma_d$  parameters.

One can see that the approximation to replace  $E_{gs}$  with  $E_g$  in the effective Hamiltonian is independent of  $\xi$  over the entire parameter range. The perturbative formula, Eq. (17), is fairly accurate for  $\xi < 0.3$ . For spontaneous fission, we can assume that  $v_{\text{eff}}$  is much smaller than  $\Delta$  and  $\Gamma_d$ . Thus, we can discuss the dynamics of spontaneous fission with the formula

$$\Gamma_f \approx \Gamma_d \xi^2. \quad (19)$$

We shall apply this to the adiabatic approximation in the next section.

#### IV. TESTING THE ADIABATIC APPROXIMATION

Most of the theoretical calculations for spontaneous and low-energy fission found in literature have been based on the adiabatic approximation, see e.g., Refs. [4–9]<sup>1</sup>. For instance, when a potential surface for fission is constructed microscopically, one often employs the constrained Hartree-Fock method to minimize the energy for a given nuclear shape. Thus only the local ground state at each deformation is taken into consideration.

A nice feature of the schematic model presented here is that it can be used to assess the validity of such approximations. In the present model, the adiabatic approximation is implemented by first diagonalizing the model Hamiltonian within subspaces of fixed  $Q$ . Then one constructs a new basis taking only the lowest energy state of each  $Q$  value. In the case of 3 pairs in 6 orbits, this approximation reduces the dimension of the Hamiltonian from 20 to 4; the states in the reduced basis have  $Q = -6, -2, 2, \text{ and } 6$ . The eigenenergies of the four states are shown by stars in Fig. 1. We note that the reduced Hamiltonian is nothing but the discrete model used in the pair hopping model<sup>2</sup> [15, 16]. In the pair hopping model, the discrete-basis representation of the Hamiltonian is transformed to a Schrödinger-like equation, from which the inertia parameter for fission is deduced. In this paper, we instead diagonalize the reduced Hamiltonian matrix as it is and compute the decay width from the eigenenergy of the ground state.

The upper panel of Fig. 4 shows a comparison of the decay width from the exact diagonalization of the original Hamiltonian matrix (the solid line) to the width in the adiabatic approximation (the dashed line) as a function of the offset  $\Delta$ , taking  $\Gamma_d = 1.2\epsilon_0$ . The ratio between the two is plotted in the lower panel. One can see that the adiabatic approximation suppresses the decay width by almost a factor of 4. One can extract a suppression factor  $S$  without carrying out the full width calculation, using instead the perturbative estimate

$$S = \frac{\Gamma_f}{\Gamma'_f} = \left( \frac{v_{eff}}{v'_{eff}} \right)^2 \quad (20)$$

where the primed quantities are the adiabatic values. This yields  $S = 4.79$  with  $v_{\text{eff}} = -0.348\epsilon_0$  and  $v'_{\text{eff}} = -0.159\epsilon_0$ .

When the barrier Hamiltonian,  $H_b$ , as well as the vectors  $\mathbf{v}_g$  and  $\mathbf{v}_d$  in Eq. (15) are expressed with the adiabatic basis, that is, the eigenstates of the Hamiltonian for a fixed value of quadrupole moment,  $Q$ , the lowest energy configurations indeed lead to the dominant contribution

<sup>1</sup> Nonadiabatic effects have also been discussed in the literature, see e.g. Refs. [10–14].

<sup>2</sup> The model has also been applied recently to  $\alpha$  decays [17–19].

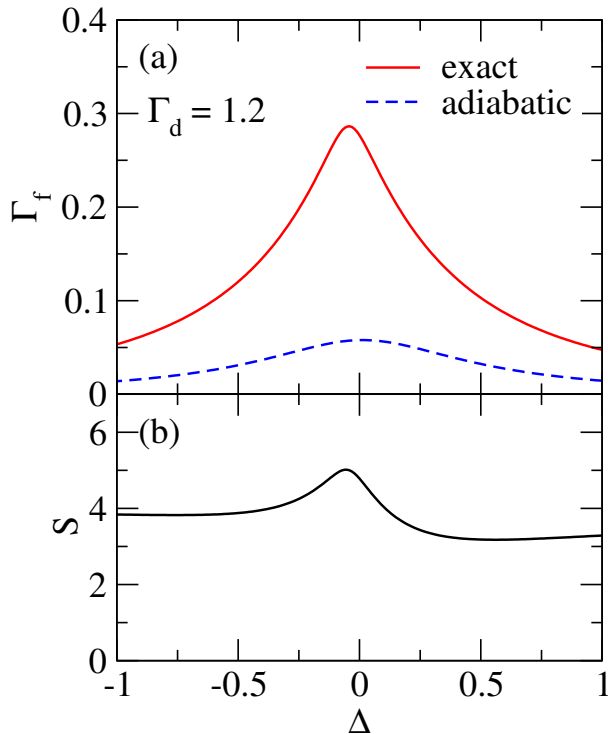


FIG. 4: The Upper panel compares the fission width from the exact diagonalization of the Hamiltonian matrix (solid line) with the adiabatic approximation (the dashed line) as a function of the offset  $\Delta$  and with  $\Gamma_d = 1.2\epsilon_0$ . Energies are measured in units of  $\epsilon_0$ . The lower panel shows the ratio  $S = \Gamma_f(\text{exact})/\Gamma_f(\text{adiabatic})$ .

in Eq. (15). However, contributions from the other configurations are not negligible, and they may provide an important contribution as a whole when the number of configurations is not small. In order to demonstrate this, Fig. 5 shows the real part of the overlap amplitude between the ground state of the original  $20 \times 20$  Hamiltonian with  $\Gamma_d = 1.2\epsilon_0$  and each of the adiabatic state as a function of the energy of the adiabatic states. The upper and the lower panels are for  $Q = -2$  and  $2$ , respectively. Here, the overlap amplitude  $O_k(Q)$  is defined as

$$O_k(Q) = \frac{\langle \phi_k(Q) | \psi_{\text{gs}} \rangle}{\sqrt{\langle \tilde{\psi}_{\text{gs}} | \psi_{\text{gs}} \rangle}}, \quad (21)$$

where  $|\phi_k(Q)\rangle$  is the  $k$ -th eigenstate of the sub-Hamiltonian spanned by the configurations with  $Q$ .  $|\psi_{\text{gs}}\rangle$  and  $|\tilde{\psi}_{\text{gs}}\rangle$  are the ground state of the non-Hermitian Hamiltonian  $H$  and its Hermitian conjugate,  $H^\dagger$ , respectively, which are normalized as  $\langle \tilde{\psi}_{\text{gs}} | \psi_{\text{gs}} \rangle = 1$  [20]. One can see that the overlap is indeed the largest for the lowest energy configuration for each  $Q$ . The overlap amplitude with the next two states are smaller than the overlap with the lowest energy state by a factor of around 2.27 for  $Q = -2$  and 2.99 for  $Q = 2$ . These are small but not negligible and contribute significantly when all the

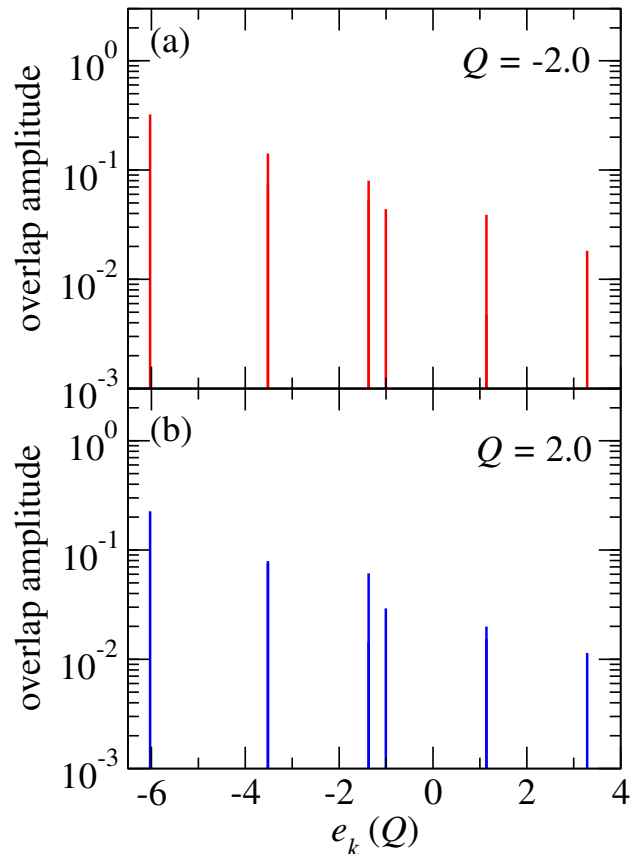


FIG. 5: The real part of the overlap amplitude between the ground state of the original  $20 \times 20$  Hamiltonian and the adiabatic basis states as a function of the energy of each of the adiabatic state. The offset and the width of the fission doorway state are set to be  $\Delta = 0.1\epsilon_0$  and  $\Gamma_d = 1.2\epsilon_0$ , respectively. The upper panel is for  $Q = -2$  while the lower panel is for  $Q = 2$ .

contributions are summed up.

It is interesting to recall that the adiabatic approximation gives the upper limit of the tunneling probability in the problem of an external potential barrier with a fixed incident energy [21, 22]. This is not the case with our Hamiltonian; here the adiabatic approximation gives a much smaller decay rate. In fact the models are so different that it should not be surprising that even qualitative features are affected.

Next we examine the sensitivity of the adiabatic approximation to physical parameters in the model: the pairing condensate  $\Delta_{\text{BCS}}$ , the barrier height  $V_B$ , and the size of the configuration space  $N_{\text{conf}}$ . Table II compares  $v_{\text{eff}}^2$  calculated with the full Hamiltonian matrix and with the adiabatic approximation. Their ratio is approximately equal to the ratio of decay widths according to Eq. (20). One sees that the adiabatic approximation becomes much better when the pairing strength is increased. Indeed, in the limit  $\epsilon_0/G \rightarrow 0$  the adiabatic

TABLE II: Comparison of the square of the effective coupling strength,  $v_{\text{eff}}^2$ , with that in the adiabatic approximation,  $(v_{\text{eff}}^{\text{ad}})^2$ , for several parameter sets of the model Hamiltonian.

Model						2×2 matrix reduction		
$(N_{\text{orb}}, N_p)$	$N_{\text{conf}}$	$V_B$	$v_Q$	$G$	$\Delta_{\text{BCS}}$	$v_{\text{eff}}^2$	$(v_{\text{eff}}^{\text{ad}})^2$	ratio
(6,6)	20	6	-5/16	0.691	1.5	0.121	0.0253	0.209
(6,6)	20	6	-5/16	1.44	4.0	21.24	21.30	1.003
(6,6)	20	10	-7/16	0.691	1.5	$1.23 \times 10^{-2}$	$2.17 \times 10^{-3}$	0.177
(8,8)	70	6	-7/32	0.585	1.5	1.18	$2.75 \times 10^{-2}$	$2.32 \times 10^{-2}$
(10,10)	252	6	-3/16	0.521	1.5	7.85	$1.75 \times 10^{-2}$	$2.22 \times 10^{-3}$

treatment is exact.

However, the adiabatic approximation is seen to fail badly as a function of  $N_{\text{conf}}$ , taking the physical parameters at the nominal values. The three cases in the table are  $(N_{\text{orb}}, N_p) = (6, 6), (8, 8)$ , and  $(10, 10)$ , and the error in the adiabatic approximation is about of factor of 0.2, 0.02, and 0.002, respectively. In these spaces the number of interior sets of given  $Q$  are 2, 3, and 4. To traverse the space from one end to the other requires an additional jump between  $Q$  values for addition set. Thus, it appears that the error cost for each  $Q$  transition is about one order of magnitude. This would be huge for a space large enough to represent the number of transitions required for an actinide nucleus.

## V. SUMMARY

We have presented a schematic model for spontaneous fission very different in spirit to previous theory. Our model is anchored in the Configuration Interaction (CI) framework of many-particle quantum mechanics. In contrast, the previous theory followed the picture of a particle tunneling under a one- or few-dimensional barrier. Since the CI space in the model is tiny compared to huge space needed for a quantitative theory, our findings are at best qualitative.

One interesting finding supporting previous studies [23] is the strong dependence of spontaneous decay rates on the strength of the pairing interaction.

The main focus of our study is the validity of the adiabatic approximation for the intermediate states, and we found a serious problem in that method. The approximation was a factor of 5 too small for Hamiltonian containing two stages of intermediate states, and about one order of magnitude smaller for each additional stage. In the physical problem, there are about 20 intermediate states [24], so clearly one needs to rethink how to deal with approximations that reduce the dimensionality to one or a few variables.

There are several directions that can be explored to make the model more realistic. One improvement over the adiabatic approximation is to simulate the least-action treatment which has been shown to increase the decay rates by several orders of magnitude [25]. Instead

of the ground state wave function in the subspaces, the model would artificially increase the pairing strength in calculating the intermediate-state wave functions. The question then arises of how much to increase the pairing strength. As a naive possibility, we have examined the change in decay rate for the (6, 6) model space, taking the pairing strength for the two intermediate wave functions that maximizes the final decay rate. Indeed, the result comes out close to the exact, but so far we have not found a good justification for the procedure.

Another problem of the model is its oversimplification of the exit from the tunneling region. In  $\alpha$ -particle decay, the exit from the tunneling region is straightforward because the barrier is due to the Coulomb potential field, and the dynamics is essentially one-dimensional barrier penetration. In contrast, spontaneous fission produces many different final states suggesting that there are many doorways to fission. Thus, the model is unrealistic in having only a single doorway. But the same criticism can be made for the traditional treatment of spontaneous fission.

Finally, the model is oversimplified in that the single-particle space only contains nucleons of the same isospin, that is, all neutrons or all protons. In principle it is straightforward to generalize the model to include both species, and the dimension  $N_{\text{conf}}$  remains manageable for the (6, 6) space in each species. It is not clear how this generalization would affect the conclusions.

The ultimate goal is to build more realistic Hamiltonians in the CI basis. The configurations can be constructed by the constrained Hartree-Fock or Hartree-Fock-Bogoliubov method [16, 26]. The configurations obtained that way are not necessarily orthogonal, but that has not posed a significant problem in other physics fields [35].

## Acknowledgments

We thank J. Dobaczewski, W. Nazarewicz and other participants in the workshop “Future of Fission Theory”, York, UK (2019) for discussions motivating this study. The work of KH was supported in part by JSPS KAKENHI Grant Number JP19K03861.

## Appendix A: Time-dependent approach

Another way to calculate fission decay rates is through a time-dependent approach [27–31]. This Appendix applies that method to our model Hamiltonian. The starting point is defining the initial wave function at time  $t = 0$ ,  $\psi(0)$ . Formally the time-dependent wave function is calculated with the time evolution operator as

$$|\psi(t)\rangle = e^{-iHt/\hbar}|\psi(0)\rangle. \quad (\text{A1})$$

where  $H$  is the Hamiltonian. Using the eigenfunctions of  $H$ ,  $|\phi_k\rangle$ , and those of  $H^\dagger$ ,  $|\tilde{\phi}_k\rangle$ , the wave function can be expressed as

$$|\psi(t)\rangle = \sum_k e^{-iE_k t/\hbar} |\phi_k\rangle \langle \tilde{\phi}_k | \psi(0)\rangle, \quad (\text{A2})$$

where the  $E_k$  are left eigenvalues of the Hamiltonian. The survival probability is computed as  $P_{\text{surv}}(t) = |\langle \psi(0) | \psi(t)\rangle|^2$ . From the survival probability, the decay width may be computed either as

$$\Gamma(t) = -\frac{\hbar}{P_{\text{surv}}(t)} \frac{dP_{\text{surv}}(t)}{dt} \equiv \Gamma_1(t), \quad (\text{A3})$$

or as

$$\Gamma(t) = -\frac{\hbar}{t} \ln P_{\text{surv}}(t) \equiv \Gamma_2(t). \quad (\text{A4})$$

If the survival probability has an exponential dependence,  $P_{\text{surv}}(t) \sim e^{-\Gamma t/\hbar}$ , both formulas yield the same decay width,  $\Gamma$ .

In the examples shown below, we take the same non-Hermitian Hamiltonian as the one given in Sec. II, taking  $\Gamma_d = 1.2\epsilon_0$ . When the initial wave function,  $\psi(0)$ , is taken as the ground state wave function of the Hamiltonian, one finds the same fission width as that obtained by the diagonalization method presented in Sec. II.

In more realistic applications it is not feasible to compute the ground state eigenfunction and some approximation to  $\psi(0)$  is introduced. There are three choices that we examine here. They are:

- i) the unperturbed ground state configuration,  $\phi_g$ ,
- ii) the ground state wave function for the real Hamiltonian with  $\Gamma_d = 0$ ,  $\psi_{\text{gs}}(\text{real})$ ,

and

- iii) the ground state wave function for the elevated-barrier Hamiltonian,  $\psi_{\text{gs}}(\text{eb})$ .

For the case iii), we follow the idea of the two-potential method [32–34], and modify the diagonal energies of the Hamiltonian in the following way: we first identify the quadrupole moment at the barrier top,  $Q_b$ , and define the maximum diagonal energy of the Hamiltonian at  $Q_b$ ,  $E_{\text{max}}(Q_b)$ . We then add a constant energy,

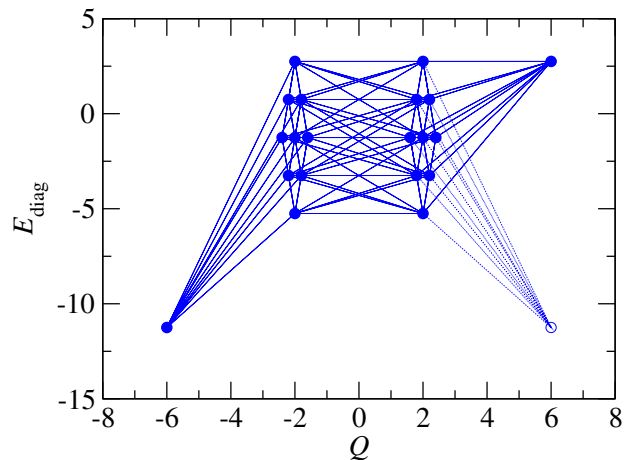


FIG. 6: A modification of the diagonal energies of the Hamiltonian for the system with 3 pairs in 6 orbitals in order to construct an initial wave function for the time-dependent approach. The diagonal energy outside the fission barrier at  $Q = 6$  is modified from the original value (denoted by the open circle) to a constant value which is set to be the same as the maximum of the diagonal energy. The solid and the dashed lines join configurations that are connected by the pairing interaction, for which the dashed lines are used to connect to the original energy point.

$E_{\text{add}}(Q) = E_{\text{max}}(Q_b) - E_{\text{max}}(Q)$ , to the diagonal energies for the configurations at  $Q > Q_b$  so that the maximum energy becomes a constant outside the barrier. This is graphically illustrated in Fig. 6 for the case with 3 pairs in 6 orbitals (we have found that the results do not significantly change even if the energy of the doorway state is set to be the same as the lowest diagonal energy at  $Q_b$ ).

Figure 7 shows the decay widths obtained by the time-dependent approach with the three different initial wave functions. The offset and the width for the doorway state are set to be  $\Delta = 0.1\epsilon_0$  and  $\Gamma_d = 1.2\epsilon_0$ , respectively. The upper and the lower panels show the decay width estimated with Eqs. (A3) and (A4), respectively. The dotted, the dashed, and the solid lines show the results with the choice i), ii), and iii) for the initial wave function, respectively. One can see that the choice i) does not provide a good result, as the decay width is highly oscillating, especially for  $\Gamma_1(t)$ . At large  $t$ , both of the choices ii) and iii) lead to the same value of the decay widths as that with the time-independent approach, which is denoted by the thin solid line. This is a natural consequence of the fact that only the component with the smallest imaginary energy survives in the time-evolution, Eq. (A2), as  $t \rightarrow \infty$ . It is worth noticing that the convergence is the fastest for  $\Gamma_1(t)$  with the choice iii), that is, the ground state wave function for a modified Hamiltonian. On the other hand, the choice ii) would be good when the width for the doorway configuration,  $\Gamma_d$ , is very small, since in this case  $\psi(\text{real})$  should be almost the same as the ground

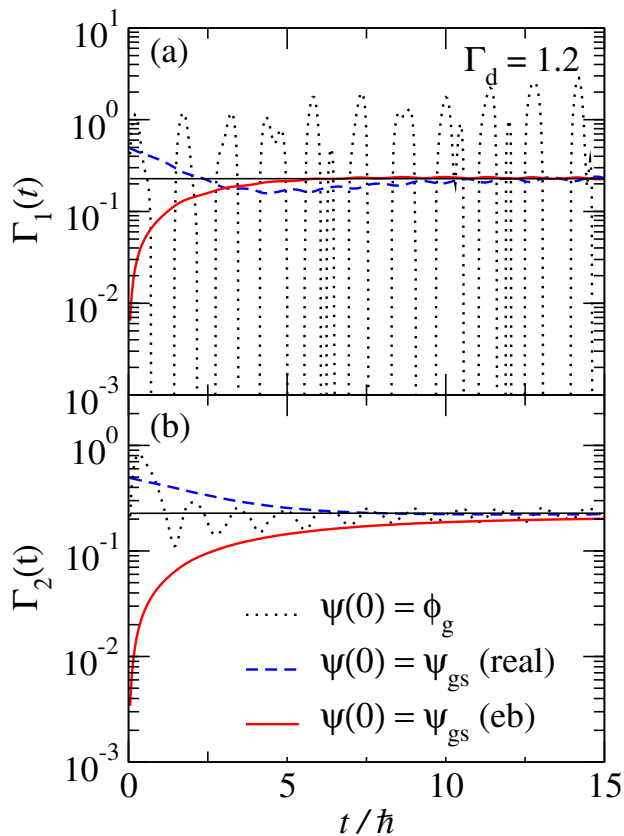


FIG. 7: The decay widths obtained with the time-dependent approach with three different initial wave functions. These are for the system with 3 pairs in 6 orbitals, with the width of the fission doorway configuration of  $\Gamma_d = 1.2\varepsilon_0$ . All the energies are measured in units of  $\varepsilon_0$ . The upper and the lower panels show the decay widths estimated by Eqs. (A3) and (A4), respectively. The dotted lines use the unperturbed ground state wave function for the initial wave function, while the dashed lines are with the ground state wave function of the real Hamiltonian with  $\Gamma_d = 0$ . The solid lines use the ground state wave function of the modified Hamiltonian shown in Fig. 6. The decay width from the time-independent approach is denoted by the thin solid lines.

state wave function of the non-Hermitian Hamiltonian.

- 
- [1] J. Dobaczewski, arXiv:1910.03924.  
[2] G.F. Bertsch, Phys. Rev. C, in press. arXiv:1912.09469.  
[3] N. Auerbach and V. Zelevinsky, Rep. Prog. Phys. **74**, 106301 (2011).  
[4] H. Goutte, J.F. Berger, P. Casoli, and D. Gogny, Phys. Rev. C **71**, 024316 (2005).  
[5] M. Warda and J.L. Egido, Phys. Rev. C **86**, 014322 (2012).  
[6] J. Sadhukhan, M. Kazurek, A. Baran, J. Dobaczewski, W. Nazarewicz, and J.A. Sheikh, Phys. Rev. C **88**, 064313 (2013).  
[7] A. Staszczak, A. Baran, and W. Nazarewicz, Phys. Rev. C **87**, 024320 (2013).  
[8] N. Schunck and L.M. Robledo, Rep. Prog. Phys. **79**, 116301 (2016).  
[9] T. Nakatsukasa, K. Matsuyanagi, M. Matsuo, and K. Yabana, Rev. Mod. Phys. **88**, 045004 (2016).  
[10] G. Schütte and L. Wilets, Nucl. Phys. **A252**, 21 (1975).  
[11] D.M. Brink, M.C. Nemes, and D. Vautherin, Ann. of Phys. (N.Y.) **147**, 171 (1983).  
[12] D. Brink and G. Schütte, Z. Phys. **A310**, 307 (1983).  
[13] R. Bernard, H. Goutte, D. Gogny, and W. Younes, Phys. Rev. C **84**, 044308 (2011).  
[14] A. Bulgac, P. Magierski, K.J. Roche, and I. Stetcu, Phys. Rev. Lett. **116**, 122504 (2016).  
[15] F. Barranco, G.F. Bertsch, R.A. Broglia, and E. Vigezzi, Nucl. Phys. **A512**, 253 (1990).  
[16] G. Bertsch and H. Flocard, Phys. Rev. C **43**, 2200 (1991).

- [17] J. Rissanen, R.M. Clark, A.O. Macchiavelli, P. Fallon, C.M. Campbell, and A. Wiens, *Phys. Rev. C* **90**, 044324 (2014).
- [18] R.M. Clark and D. Rudolph, *Phys. Rev. C* **97**, 024333 (2018).
- [19] R.M. Clark, H.L. Crawford, A.O. Macchiavelli, D. Rudolph, A. Samark-Roth, C.M. Campbell, M. Cromaz, P. Fallon, C. Morse, and C. Santamaria, *Phys. Rev. C* **99**, 024325 (2019).
- [20] P. Morse and H. Feshbach, *Methods of Theoretical Physics* (McGraw-Hill, New York, 1952), p. 884.
- [21] A.B. Balantekin and N. Takigawa, *Rev. Mod. Phys.* **70**, 77 (1998).
- [22] K. Hagino and N. Takigawa, *Prog. Theo. Phys.* **128**, 1061 (2012).
- [23] R. Rodriguez-Guzman and L.M. Robledo, *Eur. J. Phys. A* **53** 245 (2017).
- [24] G.F. Bertsch, W. Younes and L.M. Robledo, *Phys. Rev. C* **100** 024607 (2019).
- [25] R. Rodriguez-Guzman and L.M. Robledo, *Phys. Rev. C* **98** 034308 (2018).
- [26] G.F. Bertsch and W. Younes, *Ann. of Phys. (N.Y.)* **403**, 68 (2019).
- [27] O. Serot, N. Carjan, and D. Strottman, *Nucl. Phys.* **A569**, 562 (1994).
- [28] P. Talou, N. Carjan, C. Negrevergne, and D. Strottman, *Phys. Rev. C* **62**, 014609 (2000).
- [29] T. Maruyama, T. Oishi, K. Hagino, and H. Sagawa, *Phys. Rev. C* **86**, 044301 (2012).
- [30] T. Oishi, K. Hagino, and H. Sagawa, *Phys. Rev. C* **90**, 034303 (2014).
- [31] G. Scamps and K. Hagino, *Phys. Rev. C* **91**, 044606 (2015).
- [32] S.A. Gurvitz and G. Kalbermann, *Phys. Rev. Lett.* **59**, 262 (1987).
- [33] S.A. Gurvitz, *Phys. Rev. A* **38**, 1747 (1988).
- [34] S.A. Gurvitz, P.B. Semmes, W. Nazarewicz, and T. Vertse, *Phys. Rev. A* **69**, 042705 (2004).
- [35] M.B. Nardelli, *Phys. Rev. B* **60**, 7828 (1995).